IJISET - International Journal of Innovative Science, Engineering & Technology, Vol. 2 Issue 10, October 2015.
www.ijiset.com
ISSN 2348 – 7968

Modelling defects and acceptors in thin film CIGS

Demba DIALLO (ddemba00@gmail.com), Moustapha DIENG, Alain Kassine EHEMBA, Mamour SOCE, Gerome SAMBOU.

University of Cheikh Anta Diop, Dakar/Senegal, Faculty of Sciences and Techniques, Physics Department.

Abstract

Multivalent defects, e.g. double acceptors or simple acceptor, are important inmaterials used in solar cell production in general and in chalcopyrite materials in particular. We used the thin film solar cell simulation software SCAPS to enable the simulation of multivalent defects with up to five different charge states.Algorithms enabled us to simulate an arbitrary number of possible states of load. The presented solution method avoids numerical inaccuracies caused by the subtraction of two almost equal numbers. This new modelling facility is afterwards used to investigate the consequences of the multivalent character of defects for the simulation of chalcopyrite based CIGS.

Keywords: *Defects and acceptors in semiconductor CIGS, Solar cells, numerical modelling, SCAPS*

1. Introduction

Multivalent defects, i.e. defects with more than two possible charge states are important in several material systems used in solar cell production [1]–[3]. In particular for chalcopyrite materials CIGS, theoretical studies which are in good agreement with measurement results identify most of the existing defects as multivalent defects, e.g. double acceptors and simple acceptors [4]-[5]. The statistics governing this kind of defects differs from the usual Shockley-Read-Hall (SRH) statistics, for defects with only two possible charge states [1]. We used the numerical tool for simulation SCAPS for the modelling of the general-purpose defects and the states acceptors in their more general form.

2. Definitions and Assumptions

The recombination through defects is often described by the Shockley-Read-Hall (SRH) [14]-[15] statistics. The net recombination rate *U*, is considered to be the result of capture and emission processes of holes and electrons (see Figure 2.2).

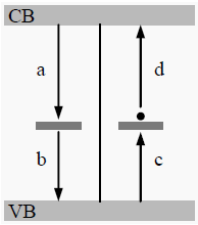

Fig.1 The basic processes involved in SRH-recombination through an acceptor defect: (a) electron capture; (b) hole emission; (c) hole capture; (d) electron emission. If the defect is in the unoccupied state (left side), processes (a) or (b) can occur leading to an occupied state (right side) and vice versa.

Partially following the notation of Sah and Shockley [1], the different charge states are designated with a subscript s representing the number of electrons on the defect. The most positive charge state corresponds then to s=0, and the most negative to s=H. The different transitions (defect levels) are designated with a superscript which is the mean value of the charge states involved. For example the density of a defect in state s is noted as Ns, and the recombination rate associated with transitions between the states s and s+1 is noted as $U^{s+1/2}$.
The different charge states are indicated at the bottom and the transitions at the top of the figure. The most positively charged state corresponds with *s* = 0 in this example.

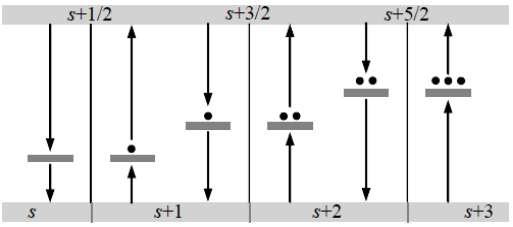

Fig.2 The basic processes involved in recombination through a multivalent defect with four different charge states (*N* = 4).

The arrows represent capture and emission processes in a similar way as in Fig 1. The net electron and hole capture rates are noted as $U_n^{s+1/2}$ and $U_p^{s+1/2}$ Eq (1).

$$\begin{cases} U_n^{s+1/2} = nc_n^{s+1/2}N_s - e_n^{s+1/2}N_{s+1} \\ U_p^{s+1/2} = pc_p^{s+1/2}N_{s+1} - e_p^{s+1/2}N_s \end{cases} \quad (1)$$

With c_n and c_p the electron and hole capture constants. In order to calculate the emission coefficients (e_n, e_p) the theory of detailed balance has to be applied. For

ISSN 2348 – 7968

multivalent defects the grand partition function has to be used instead and take into account possible degeneracies [10]-[11], leading to the Eq (2).

$$\begin{cases} e_n^{s+1/2} = N_c c_n^{s+1/2} \dfrac{g_s}{g_{s+1}} \exp\left(-\dfrac{E_c - E_t^{s+1/2}}{kT} \right) \\ e_p^{s+1/2} = N_V c_p^{s+1/2} \dfrac{g_{s+1}}{g_s} \exp\left(-\dfrac{E_c - E_t^{s+1/2}}{kT} \right) \end{cases} \quad (2)$$

3. Numerical Procedures and Algorithms

In order to calculate the occupation probabilities of the different defect levels continuity has to be Eq (3).

$$\frac{\partial N_s}{\partial t} = U_n^{s-1/2} - U_n^{s+1/2} - U_p^{s-1/2} + U_p^{s+1/2} \quad (3)$$

This expression doesn't hold for the most negative and positive charged states, e.g. for s=0 and s=1, it should be replaced respectively with Eq (4) and Eq (5).

$$\frac{\partial N_0}{\partial t} = -U_n^{1/2} + U_p^{1/2} \quad (4)$$

$$\frac{\partial N_1}{\partial t} = U_n^{1/2} - U_n^{3/2} - U_p^{1/2} + U_p^{3/2} \quad (5)$$

4. Results and discussions

To illustrate the importance of correct multivalent modelling, we start from the 'NUMOS CIGS baseline.def' model [13], which is distributed together with the installation package of SCAPS, and which is a good representative for a CIGS thin film solar cell structure. This structure consists of a 3 µm wide CIGS absorber layer, together with a 50 nm CdS buffer layer and a ZnO window layer.

To illustrate the importance of correct multivalent modelling, we start from the 'NUMOS CIGS baseline.def' model [13], which is distributed together with the installation package of SCAPS, and which is a good representative for a CIGS thin film solar cell structure. This structure consists of a 3µm wide CIGS absorber layer, together with a 50 nm CdS buffer layer and a ZnO window layer. In the p-type absorber layer, a band gap of 1.1 eV and a shallow doping density of 2.1016 cm^{-3} is assumed.

In this layer, we present a defect of the type charges: double acceptor (possible charge states 2-, 1-, 0), with energy levels 0.60 eV and 0.60 eV above the valence band level and with a defect density of $1.77.10^{13}$ cm^{-3}, the capture constants are shown in Table 1.

Table 1 : Overview of the capture constants used for the SCAPS model.

Defect (level)	Level 1 (0/—)	Level 2 (—/2—)
c_n (cm^3/s)	5.10^{-12}	10^{-19}
c_p (cm^3/s)	10^{-15}	10^{-19}

The results are compared with the results of simulation of the same structure but where the defect of double acceptor in the layer of shock absorber was replaced with a defect of simple acceptor, taking account of the degeneration as shown in the equations.All simulations are carried out to 300 K. Results of simulation the Current density Shockley, Read, Hall (recombination) as a function of the Voltage (J_{SRH}-V) characteristic under AM1_5G 1 sun.spe illumination conditions are shown in the fig. 3.

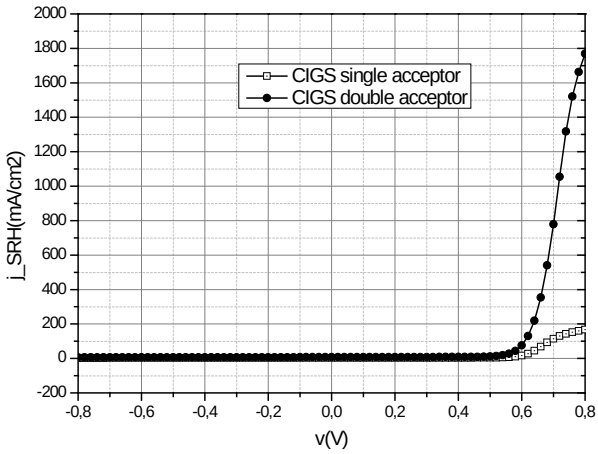

Fig.3 SCAPS simulation of the Current density Shockley, Read, Hall (recombination) as a function of the Voltage (J_{SRH}-V) characteristic under AM1_5G 1 sun.spe illumination conditions. Comparison of the models with a defect single acceptor and a defect double acceptor.

It is shown that by increasing the thickness from -0.8V to 0.8V, J_{SRH} is constant and after 0.45V, J_{SRH} increases near exponentially. From the simulation results it was found that by increasing cell layers the states acceptors of the defects of a layer CIGS, there is an exchange rigorously on the level of the electric property J_{SRH} is 175 mA/cm^2 for the CIGS single acceptor and 1800 mA/cm^2 for the CIGS doubles acceptor against the tension applied of 0.8V.

ISSN 2348 – 7968

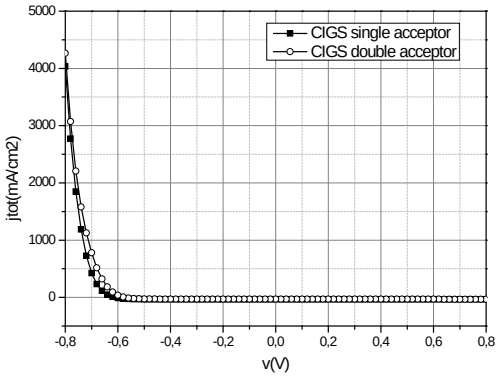

Fig.4 SCAPS simulation of the Total current density as a function of the voltage (J_{tot} -V) characteristic under AM1_5G 1 sun.spe illumination conditions. Comparison of the models with a defect single acceptor and a defect double acceptor.

The total current as a function of voltage under illumination is shown in the Fig.4. It includes series resistance, shunt conductance and the saturation current density for the recombination mechanism under illumination. We notice that the total current decreases gradually when the tension applied increases. The results of simulation give with the CIGS single acceptor J_{tot}=4032.27 mA/cm^2 and the CIGS double acceptor J_{tot}=4265.49 mA/cm^2.

From Fig.5, we can see that at low voltage, the capacitance increases with voltage. It then goes through a maximum and quickly drops for the two curves. we have maximum values of the capacitance of 39.8125 nF/cm^2 and 39.7775 nF/cm^2 respectively for the single acceptor and double aceptor at a frequency of 10^5 Hz .

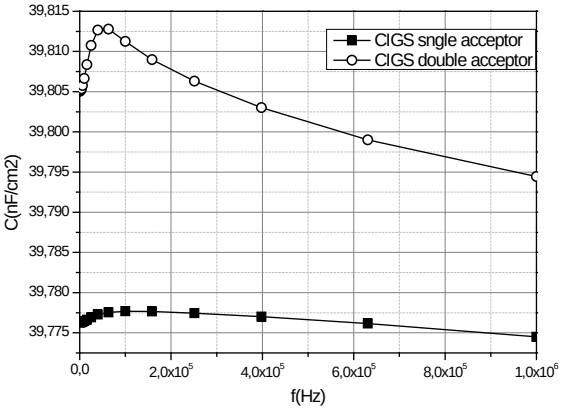

Fig.5 SCAPS simulation of the capacitance as a function of the frequency (C-f) characteristic under AM1_5G 1 sun.spe illumination conditions. Comparison of the models with a defect single acceptor and a defect double acceptor.

Moreover under the polarization of inversion conditions catch of this agreement. Under downstream polarized conditions the agreement breaks up, except very at high frequencies where the defects do not contribute any more to the capacity.

4. Conclusions

The examples given above illustrate the numerical simulation program SCAPS is a valuable tool in modelling defectthin film solar cells based on CIGS. The fan of possible input parameters is so wide that one cannot be sure that there does not exist another set of parameters which will yield agreement between measurement and calculation which could be judged equally well as the one in Figs.4 and 5. This method is employed to show that being unaware of the general-purpose nature of a defect. Also, the choice of the input parameter set should be guided by the outcome of independent non-electrical measurements.

References

[1] C.-T. Sah, W. Shockley, Phys. Rev. 109 (4) (1958) 1103.
[2] A. Milnes, John Wiley and sons "Deep Impurities in Semiconductors", New York, 1973.
[3] R.E.I. Schropp, M. Zeman, "Amorphous and Microcrystalline Silicon Solar cells", Kluwer academic publishers, Norwell, 1998.
[4] S. Siebentritt, U. Rau, "Wide-Gap Chalcopyrites", Springer-Verlag, Berlin Heidelberg, 2006.
[5] S.B. Zhang, S.H. Wei, A. Zunger, Phys. Rev. B 57 (16) (1997) 9642.
[6] A. Froitzheim, R. Stangl, M. Kriegel, L. Elstner, W. Fuhs, "Proceedings of the 3rd World conference on Photovoltaic Solar Energy Conversion", Osaka (J), 2003, 1PD3-34.
[7] Developed at Pennsylvania State University under the direction of S.J.Fonash, see:http://www.ampsmodeling.org / default.htm (last accessed July 2010).
[8] F. Smole, J. Krč, J. Furlan, Sol. Eergy Mater. Sol. Cells 34 (1994) 385.
[9] M. Burgelman, P. Nollet, S. Degrave, "Modelling polycrystalline semiconductor solar cells", Thin Solid Films 361–362 (2000) 527.
[10] D.C. Look, Phys. Rev. B 24 (10) (1981) 5852.
[11] W. Shockley, J.T. Last, Phys. Rev. 107 (2) (1957) 392.
[12] A. Niemegeers, S. Gillis, M. Burgelman, in: J. Schmid, H.A. Ossenbrink, P. Helm, H. Ehmann, E.D. Dunlop (Eds.), "Proceedings of the 2nd World conference on Photovoltaic Solar Energy Conversion", Vienna (A), 1998, p.672.
[13] M. Burgelman, J. Verschraegen, B. Minnaert, J. Marlein, in M. Burgelman, M. Topič (Eds.), "Proceedings of NUMOS", Gent, B., 2007, p.357
[14] K. Decock, S. Khelifi, M. Burgelman, "Uniform reference structures to assess the benefit of grading in thin film solar cell structures", Proceedings of the 25th European Photovoltaic Solar Energy Conference, Valencia, 2010, pp. 3323-3326.
[15] K. Decock, J. Lauwaert, M. Burgelman, "Modelling thin film solar cells with graded band gap", Proceedings of the 45th International conference on Microelectronics devices and technologies, Postojna, 2009, pp. 245-249.